Anisotropic diffusion in benzene: ^{13}C NMR study

Terry Gullion and Mark S. Conradi
College of William and Mary, Department of Physics, Williamsburg, Virginia 23185
(Received 10 June 1985)

We report a ^{13}C NMR measurement of the three distinct diffusion jump rates present in solid benzene (orthorhombic). Diffusion jumps from one a-b plane to another are found to be preferred over jumps within any one plane. The rates of the two kinds of out-of-plane jumps are unexpectedly found to be nearly equal. These findings should serve as a rigorous test of any calculations of diffusion in solid benzene. We have also measured the temperature dependence of the average of the three rates. Our results for the prefactor ω_0 agree with previous NMR determinations, but disagree with radiotracer data.

INTRODUCTION

In a cubic crystal, any given molecule is surrounded by n exactly equivalent immediate neighbors ($n=12$ for fcc, $n=8$ for bcc, $n=6$ for sc). Thus, because all the immediate neighbors are equivalent, there is only one rate of jump diffusion in such a solid. Typically, the rate at any temperature and/or the activation energy of diffusion are the only information available for comparison with theory. Much more information is available in orthorhombic benzene.[1,2] Since the twelve immediate neighbors of a given molecule fall into three groups of four each (nearest, intermediate, and most distant), there are three distinct diffusion jump rates possible in solid benzene. We report here a ^{13}C high-resolution solid-state NMR measurement of the three jump rates; our results should provide a more rigorous test of any theory or model of diffusion in simple solids.

Early evidence of diffusion processes in benzene came from a proton T_{1D} (ultraslow motion) NMR experiment.[3] The data were later explained by O'Reilly and Peterson as being due to self-diffusion.[4] A radiotracer study by Fox and Sherwood directly observed the diffusion in benzene.[5] They concluded that the diffusion is thermally activated [$\omega_J=\omega_0\exp(-\Delta E/k_BT)$] with an activation energy ΔE of 23.1 kcal/mole, and with a prefactor ω_0 equal to 2.80×10^{24} sec^{-1}. In this paper we convert[6] the prefactor D_0 to ω_0 using $\omega_0=12D_0/a^2$, where $a=7.88$ Å. A series of NMR powder-sample experiments by Noack and coworkers produced results in disagreement with the tracer data.[6,7] Their $T_{1\rho}$ (rotating-frame longitudinal relaxation) experiment measured[6] the rate of motion and found an activation energy equal to 22.46 kcal/mole, but the prefactor was determined to be 3.17×10^{20} sec^{-1}. A subsequent low-field study of the proton T_1 yielded similar results:[7] $\Delta E=22.8$ kcal/mole and $\omega_0=7.87\times10^{20}$ sec^{-1}. The two NMR values of ω_0 may be considered in good agreement since the determinations of ω_0 involve long extrapolation to infinite temperature. Thus, the NMR and tracer experiments find the same temperature variation (activation energy) of the diffusion but they disagree by almost four orders of magnitude on the absolute rate at any temperature. The pressure dependence of the proton $T_{1\rho}$ has been examined and implies an activation volume within the range expected for vacancy diffusion.[8] The $T_{1\rho}$ data at zero pressure agree with the results of Noack *et al.*[6] Hence, the first goal of this work is to resolve the disagreement over the *rate* of diffusion in benzene.

Solid benzene is an orientationally ordered solid consisting of four sublattices.[1,2] When a molecule diffuses, it moves to a new sublattice and reorients accordingly. This reorientation will change the resonance frequency of the ^{13}C spins on the diffusing molecule because of the anisotropic chemical shift. The diffusion process is monitored in the experiments described here by following changes in the ^{13}C resonance frequency caused by the reorientation of the molecules. The powder ^{13}C experiments described here measure the mean of the three jump rates mentioned above.

The second and main goal of this work is to individually measure the three jump rates. These are determined from a single-crystal experiment using the saturation transfer technique. The results provide an unusually detailed picture of diffusion in benzene.

EXPERIMENTAL

Experiments were done on polycrystalline and single-crystal samples prepared from reagent-grade benzene. The polycrystalline samples were prepared by bubbling argon gas through the liquid to remove dissolved oxygen. Next, a thermocouple was dipped into the liquid and then the tube was epoxy sealed with one atmosphere of argon gas. To obtain a good powder, the sample was rapidly cooled in liquid nitrogen and promptly placed into the already cold NMR probe.

Ten single-crystal samples were prepared but only one was used throughout the single-crystal portion of this work. Nitrogen gas was bubbled through the benzene to remove dissolved oxygen; then, four freeze-pump-thaw cycles were performed. The sample tube was then backfilled with nitrogen gas at 0.8 atmospheres of pressure. The addition of gas provided good thermal contact and also prevented electrical breakdown from the high rf voltage encountered in pulsed NMR. The sample was cooled with

 ©1985 The American Physical Society

liquid nitrogen and the sample tube was then sealed. The crystal was grown using the Bridgman technique;[9] the sample tube was dropped from room temperature into an ice-water bath (benzene melts at 278.6 K) at a rate of 0.15 in./h for a total of 6 h, producing very clear specimens. Sample quality was considered good since the width of the individual ^{13}C NMR lines was approximately 160 Hz, with 30 Hz of this due to ^{13}C-^{13}C dipolar interactions. A small mosaic spread in the crystal is believed to be responsible for the remaining width of the lines.

A simple goniometer was used in the single-crystal experiment. The sample tube could be rotated about an axis perpendicular to the Zeeman field. This arrangement was used to assign the four sharp lines in the single-crystal spectrum to the four sublattices by comparison with x-ray data[1,2] for the molecular orientations (see the Appendix).

The sample temperature was controlled by blowing thermostated nitrogen gas over the sample tube. Copper-constantan thermocouples were used to measure the temperature. The temperatures measured were accurate to within ± 1 K.

The spectrometer has been described in detail elsewhere.[10,11] Briefly, a single-coil, double-resonance probe was used allowing the enhancement of the ^{13}C signal by cross polarization[12,13] and allowing elimination of the ^{1}H-^{13}C dipolar interaction by proton decoupling.[13] The proton resonance frequency was 82.9 Mhz. Ninety-degree pulse lengths were 3.6 μ sec for protons and 5.1 μ sec for carbon. Data were acquired by a transient digitizer; a microcomputer was used to time the pulse sequences and to average and analyze the data.

THEORY

Solid benzene has an orthorhombic crystal structure with space group *Pbca* (Fig. 1).[1,2,14] All three crystal axes have different lengths so the molecular centers sit on a stretched fcc lattice. There are four sublattices; any particular molecule is surrounded by twelve immediate neighbors, four from each of the three *other* sublattices. As shown in Fig. 1, the distances to these twelve immediate neighbors are not equal. Labeling the sublattices 1, 2, 3, and 4, the distances d_{12}, d_{13}, and d_{14} are all different. Thus, one expects the rates of jump diffusion (ω_{12}, ω_{13}, and ω_{14}) between these sublattices to be all different. We note that the symmetry of the crystal requires that $\omega_{12}=\omega_{34}$, $\omega_{13}=\omega_{24}$, and $\omega_{14}=\omega_{23}$; the usual detailed balance condition dictates that $\omega_{ab}=\omega_{ba}$.

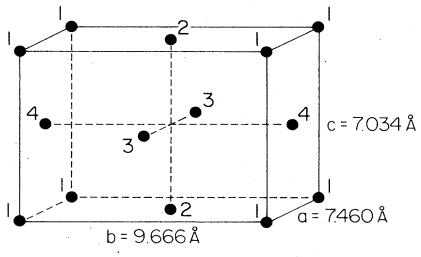

Intermolecular Distance (Å)

	2	3	4
1	6.10	5.97	5.13
2		5.13	5.97
3			6.10

FIG. 1. Location of the molecular centers in the orthorhombic structure of benzene. The positions are the corners and face centers of a stretched cube ($a \neq b \neq c$). The four sublattices are numbered. The distances of the immediate neighbors are given in the table.

Many years ago, Andrew and Eades looked at solid benzene with NMR.[15] From their second-moment and T_1 studies, they found very rapid sixfold reorientations about the molecular sixfold axes above 120 K; the reorientation rate near the melt was found to be $\approx 10^{11}$ sec^{-1}. We note that for the purposes of NMR, this sixfold reorientation can be considered to be uniform rotation.[16] The reorientations cause all six carbon sites on a molecule to be magnetically equivalent.

In the presence of proton decoupling (as used here), the ^{13}C line is dominated by chemical shift anisotropy. The chemical shift tensor is made uniaxially symmetric by the averaging from the rapid sixfold reorientations;[17] the unique symmetry axis of the tensor is the molecular sixfold axis. Because all the molecules on any sublattice are oriented parallel and because the rapid sixfold reorientations make all carbons on a molecule magnetically equivalent, all carbons on any one sublattice are magnetically equivalent. The resonance frequency ω is given by

$$\omega=\omega_0[1+\sigma_\perp+(\sigma_{||}-\sigma_\perp)\cos^2\gamma_z]\,, \tag{1}$$

where $\sigma_{||}$ and $\sigma_\perp$ are the principal elements of the shift tensor (averaged by the sixfold reorientations), and γ_z is the angle between the external field $\mathbf{H}_0$ and the normal to the molecular plane. Because the molecules on the four sublattices are oriented differently and will have different γ_z, the ^{13}C spectrum of a single crystal (or crystallite) will be four sharp lines, one from each sublattice.

When a molecule diffuses, it jumps to a new sublattice. Consequently, a ^{13}C spin on a diffusing molecule changes its resonance frequency. This situation is similar to the famous problem of chemical exchange in magnetic resonance.[16,18] The techniques for studying diffusion in benzene are likewise similar to those used to study chemical exchange: selective saturation and subsequent saturation transfer, spin echoes, and stimulated echoes.

POLYCRYSTALLINE EXPERIMENTS: RESULTS AND DISCUSSION

Spin-echo and stimulated-echo (Ref. 19) ^{13}C experiments were performed on polycrystalline samples containing naturally abundant ^{13}C. These pulse sequences have been applied to study diffusion in other orientationally ordered solids and have been more fully described.[20,21]

The spin-echo experiment consists of the pulse sequence 90_x-τ-180_y to measure the transverse relaxation time T_2. T_2 was determined by the dependence of the echo amplitude on the time 2τ. The signal-to-noise ratio was improved by averaging 20 echoes, and coherent noise was eliminated by phase alternation of the first pulse.

During the time between the two pulses, the spin isochromats dephase due to the chemical shift anisotropy. The 180° pulse at time τ inverts the transverse magnetiza-

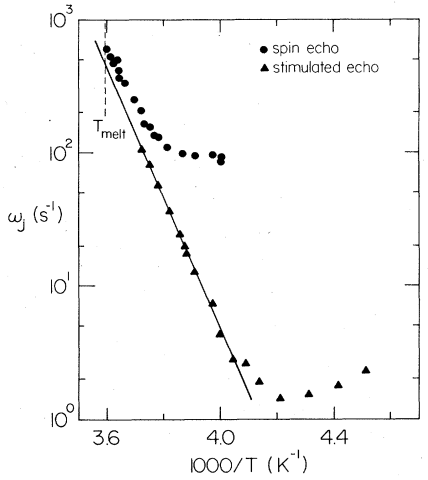

FIG. 2. Decay rate of ^{13}C spin echoes and stimulated echoes in polycrystalline benzene. The spin-echo data (circles) are T_2^{-1} values. At high temperatures, T_2^{-1} is just the diffusion jump rate ω_j averaged over the three kinds of jumps. The stimulated-echo data (triangles) are ω_j values obtained by fitting Eq. (2) to the experimental decays. At low temperatures, the spin- and stimulated-echo data are limited by spin-spin and spin-lattice effects, respectively. The straight line corresponds to thermally activated diffusion (see text).

tion so that the isochromats will refocus at time 2τ. However, only those isochromats that have remained at the same frequency (and hence orientation) during the time 2τ will contribute to the echo. Those isochromats that change frequency (due to diffusion) dephase so that their contribution to the echo is essentially zero. This is true because the system is always in the slow-jump limit ($\omega_j < \Delta\omega_{RL}$, where $\Delta\omega_{RL}$ is the powder-pattern linewidth, $(2\pi)3.8\times10^3$ sec^{-1}; the jumps are never fast enough to narrow the line).[16,18] Diffusion causes the echo amplitude to decay as $\exp(-2\tau/\tau_j)$, so the phenomenological time T_2 equals the mean time between jumps, $\tau_j(\tau_j \equiv \omega_j^{-1})$. There is also a spin-spin contribution to the decay of the echoes from the ^{13}C-^{13}C dipolar coupling. This contribution should be temperature independent and will yield an approximately Gaussian echo envelope.

The spin-echo data are shown in Fig. 2. At high temperatures, the T_2 data are thermally activated due to diffusion; T_2 should equal τ_j. At low temperatures, T_2 is determined by spin-spin interactions. A "dilute lattice" calculation[22] predicts the ^{13}C-^{13}C linewidth in natural abundance to be about 30 Hz full width at half maximum (FWHM); this in turn predicts a limiting value of T_2 of about 10 msec, in agreement with the low-temperature T_2 data. Clearly, the T_2 measurement can only determine the rate of jumps when the jump rate is larger than the ^{13}C-^{13}C spin-spin interaction.

Stimulated echoes were generated by a 90_x-τ-90_x-T-90 pulse sequence. Twenty averages were used to improve the signal-to-noise ratio, and phase alternation of the first pulse was used to eliminate coherent noise. Stimulated echoes were used because they can measure motions

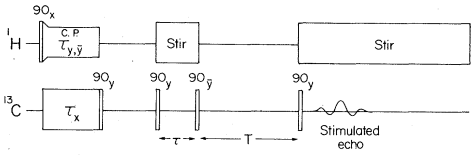

FIG. 3. Complete pulse sequence for the stimulated-echo experiment on polycrystalline benzene. A cross-polarization begins the sequence; the three 90° ^{13}C pulses produce a stimulated echo. The protons are stirred whenever transverse ^{13}C magnetization is present.

slower than those detectable by two-pulse spin-echo experiments.

The stimulated echo occurs at a time τ after the third pulse. The only isochromats which contribute to the echo formation are those whose initial frequency (from $t=0$ to τ) and final frequency (from $t=T+\tau$ to $T+2\tau$) are equal. Thus, only isochromats that remain at their initial frequency *or* return to their initial frequency are present in the echo. It is important to note that the stimulated echo involves transverse magnetization only during a total interval of 2τ (here, τ was usually 1500 μ sec; other values of τ yielded the same results). During the long waiting period T, the magnetization is stored along the $\pm Z$ axis. Thus, the time T is limited only by the spin-lattice relaxation time T_1; hence, very slow motions can be measured. In benzene, T_1 is of the order of 2 sec. The complete pulse sequence for this experiment is shown in Fig. 3.

The amplitude of the stimulated echo is[20,21]

$$A(T)=\tfrac{3}{4}\exp(-\tfrac{4}{3}\omega_j T)+\tfrac{1}{4}\ . \qquad (2)$$

The one-quarter base line occurs because there is a $\frac{1}{4}$ chance of a diffusing molecule returning to its original sublattice. Note that if diffusion occurred only between pairs of the four sublattices (e.g., if only ω_{12} and ω_{34} were nonzero), then the base line would be $\frac{1}{2}$. Figure 4 shows

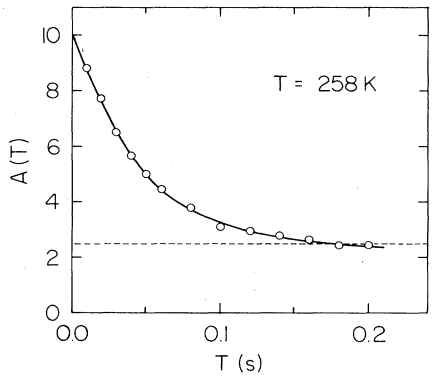

FIG. 4. Amplitude of the stimulated echo as a function of the diffusion time T in polycrystalline benzene. The pulse sequence of Fig. 3 was used. The echoes decay to a relative base line of 0.25, as indicated by the dashed line. This demonstrates that motion occurs between all four sublattices. The solid curve is an eye guide.

the stimulated-echo amplitude as a function of T at 258 K. Clearly, the base line is $\frac{1}{4}$, which implies that diffusion does occur between all sublattices. In detail this indicates that no more than one of the rates ω_{12}, ω_{13}, or ω_{14} is zero (see below).

The jump rate from stimulated echoes as a function of temperature is shown in Fig. 2. At high temperature the rate is thermally activated, but at low temperature, T_1 processes dominate the decay of the echo amplitude. At the low temperatures the echo envelope $A(T)$ decays to zero, as expected. The low-temperature limiting values of the stimulated-echo decay rate are near 1 sec^{-1}, in fair agreement with the ^{13}C T_1 in benzene (measured independently in this laboratory).

A best-fit line to the jump-rate data from the stimulated echoes is drawn in Fig. 2. The spin-echo data are offset slightly from the straight-line extension of the stimulated-echo data, but it appears that they converge in the limit of large ω_j. This effect has been seen previously[20,21] and probably reflects the spin-spin contribution to T_2^{-1}. We have fitted to the stimulated-echo data and not the spin-echo data because of the longer range of the stimulated-echo data and because of the cleaner interpretation of the experiment. The straight line in Fig. 2 follows from the thermal activation expression $\omega_j=\omega_0\exp(-\Delta E/k_BT)$, with an activation energy ΔE of 22.84 kcal/mole and with a prefactor ω_0 of 4.12×10^{20} sec^{-1}. ΔE agrees very well with both the previous NMR work[6,7] and the radiotracer work.[5] However, the prefactor agrees only with the previous NMR results.

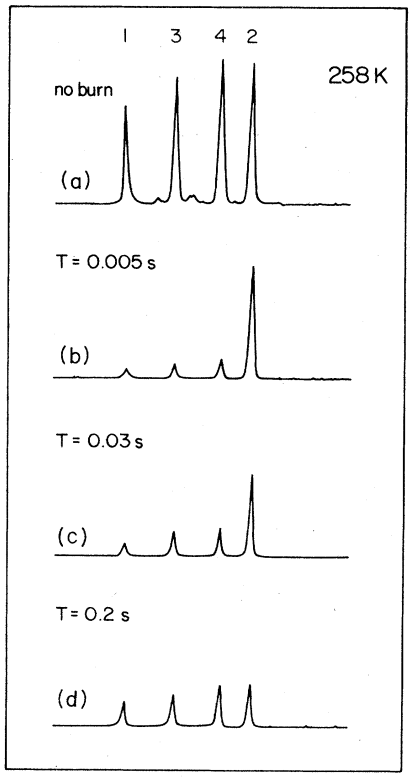

FIG. 5. Proton-decoupled ^{13}C spectra from a single crystal of benzene. (a) The spectrum without selective saturation. The four lines are from the four sublattices. Lines 1 and 2 are 2000 Hz apart. The small peaks are from small crystals. The variation of the line heights is due to a small variation in linewidths, not evident in the figure. (b) The spectrum 5 msec after saturating three of the lines. (c) After 30 msec, some magnetization transfer has occurred via diffusion. (d) After 200 msec, the lines have nearly equal intensities.

SINGLE-CRYSTAL EXPERIMENTS: RESULTS AND DISCUSSION

For an arbitrary orientation of magnetic field, there are four lines in the ^{13}C proton-decoupled spectrum, one line for each sublattice. This is shown in Fig. 5(a). Each of the four lines was assigned to one of the four sublattices by measuring the frequencies of the lines as the crystal was rotated in the goniometer (see Appendix for details). Hereafter, the lines are labeled in accordance with Cox's labeling of the sublattices.[1,2]

At the temperature used for the single-crystal experiments (258 K), the jump rates are smaller than 10 sec^{-1}. The only effect of these slow jumps upon the fully relaxed spectrum is a negligible amount of lifetime broadening ($\approx$3 Hz FWHM).[16,18] Thus, the selective saturation experiments performed on the single crystal may be described entirely in terms of the *longitudinal* magnetizations M_j ($j=1$, 2, 3, or 4) of the four sublattices. The time evolution of the magnetizations M_j is given by the master rate equations; for the system here, these equations are

$$\frac{dM_a}{dt}=\frac{M_0-M_a}{T_1}-(\omega_{ab}M_a+\omega_{ac}M_a+\omega_{ad}M_a)$$
$$+(\omega_{ab}M_b+\omega_{ac}M_c+\omega_{ad}M_d)\,, \qquad (3)$$

where $a,b,c,d=1,2,3,4$ in any order. The first term is spin-lattice relaxation; we have assumed equal thermal equilibrium magnetizations for the four lines because they involve equal numbers of spins. The relaxation times T_1 are also assumed equal; this is a fair approximation.[23] The second set of terms expresses the effect of sublattice a magnetization jumping by diffusion to the other sublattices. The third term contains the magnetization brought to the line a from the other lines. We remark again that there are only three distinct jump rates because of the symmetry of the crystal: $\omega_{12}=\omega_{34}$, etc.

The selective saturation experiment was carried out with the 90_y-t-$90_{\bar{y}}$-T-90_y pulse sequence. The first two pulses make up the "preparation" part of the sequence; their function is to saturate all the lines except the one on carrier frequency. Considering a single isochromat of initial magnetization M_0 whose frequency relative to the carrier is $\Delta\omega$, the magnetization after the first two pulses will be

$$M=M_0\cos(\Delta\omega t)\,. \qquad (4)$$

For every value of T studied, the free-induction decays following the third pulse were simply added up while t was incremented from 100 μsec to 6000 μsec in 60 equal

steps. By virtue of linearity, the net effect is as though one added the magnetizations in Eq. (4) above for all the values of t. Because

$$\int_0^\infty \cos(\omega t)dt = \pi\delta(\omega) ,$$

only the magnetization of the line *at* the carrier frequency is present in the sum over Eq. (4). This experiment is the $\omega_1=0$ slice of a related two-dimensional Fourier-transform experiment.[24] The spectrum of Fig. 5(b) shows the result of this pulse sequence. The time T is so short that little relaxation and magnetization transfer have occurred; only the line at the carrier frequency is not saturated.

During the time T, diffusion occurs with the accompanying magnetization transfer, as given by Eq. (3). The longitudinal magnetizations just before the third pulse are inspected by the 90° pulse; the resulting free-induction decay is stored, averaged, and later Fourier transformed. The spectra in Figs. 5(b), 5(c), and 5(d) show the time (T) evolution of the magnetizations. Clearly, the saturated lines recover as the initially unsaturated line decreases in intensity. The total integrated intensity of the four lines is essentially constant, showing that spin-lattice relaxation is only a small effect here. The evolution of the line intensities is dominated by the magnetization transfer given by the second and third terms of Eq. (3).

The time evolution of the four lines is shown more clearly in Fig. 6. An approximate description of the recoveries is that lines 3 and 4 recover at the same rate, while line 1 recovers more slowly. We note that if ω_{12} were zero, line 1 would *still* recover: magnetization from line 2 could transfer to line 1 indirectly through lines 3 or 4 as intermediates (i.e., $\omega_{12}=0$ but $\omega_{13}\neq 0\neq\omega_{32}$). Thus, one expects in this case that line 1 would recover twice as slowly as lines 3 and 4, because two jumps are needed to go from 2 to 1. Hence, the time evolutions in Fig. 6 are roughly in accord with $\omega_{23}=\omega_{24}$ and $\omega_{12}=0$.

We have generated numerical solutions to Eq. (3), using the above ω_{ab} as starting points. T_1 was determined to be

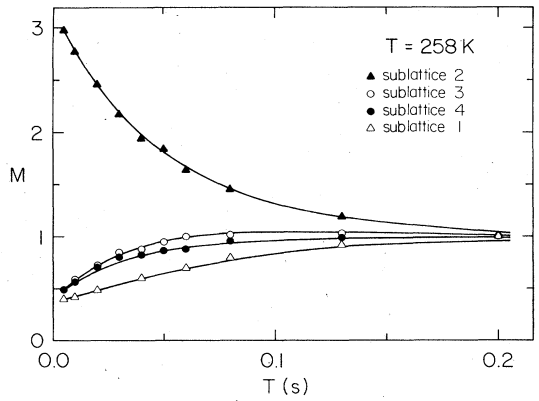

FIG. 6. Time evolution of the longitudinal magnetizations following selective saturation of lines 1, 3, and 4. The jump rates ω_{23} and ω_{24} are nearly equal; ω_{21} is smaller. The data are from Fig. 5 and are shown as symbols. The solid curves are a fit to the data using Eq. (3) (see text for values of ω_{ab}).

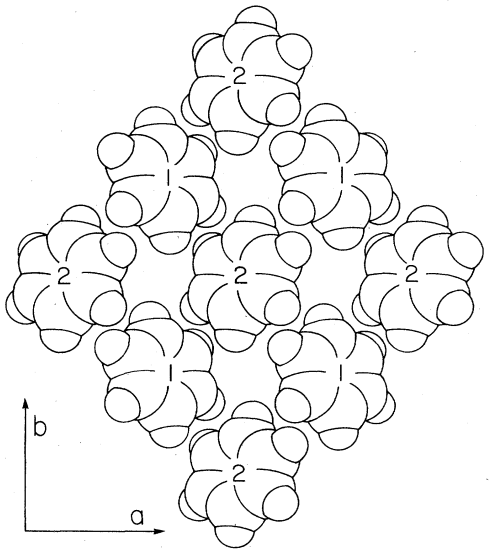

FIG. 7. From Ref. 1. One layer of the benzene structure parallel to the a-b plane is shown. The adjacent layers contain only molecules of sublattices 3 and 4. Our results indicate that diffusion between planes is faster than diffusion within a plane.

2.2 sec from a separate nonselective experiment. The comparison of the data and the numerical solutions clearly show that $\omega_{14}>\omega_{13}$ and $\omega_{12}\neq 0$. Our best fit to the data is shown in Fig. 6 and was obtained with $\omega_{12}=1.25$ sec^{-1}, $\omega_{13}=6.50$ sec^{-1}, and $\omega_{14}=8.25$ sec^{-1}. The uncertainty on each rate is ± 0.50 sec^{-1}. We have repeated the experiment with each of the other three lines at the carrier frequency. In each case the results agree with the above ω_{ab} values and the symmetry relations: $\omega_{12}=\omega_{34}$, etc. It should be noted that $T_1\omega_j \gg 1$; hence, the spin-lattice relaxation is always a small effect and appears in the data only at long times when the lines have obtained a common spin temperature. Thus, any variation of T_1 amongst the four lines[23] neglected in Eq. (3) will not matter.

The crystal structure of benzene has been regarded as a layered structure by Cox.[1,2] Figure 7 is a reproduction of Fig. 3 of Ref. 1. The structure consists of sheets parallel to the a-b plane containing molecules of sublattices 1 and 2 alternating with sheets containing molecules of sublattices 3 and 4. The molecular planes are all tipped out of the sheets. In any one sheet, the benzene molecules are packed so that they are intermeshed like beveled gears. Since the intermeshing defines rings of four molecules, it was suggested[1,2] that the sixfold reorientations would be highly correlated, at least over short distances.

In terms of Cox's picture of benzene, our results mean that jumps carrying a molecule from one sheet to a different sheet (sublattices $1\rightarrow 3$, $1\rightarrow 4$, etc.) occur more rapidly than jumps entirely within a single sheet (sublattices $1\rightarrow 2$, $3\rightarrow 4$). Furthermore, the rates ω_{13} and ω_{14} of out-of-plane jumps are nearly equal. If one assumes that ω_{13} and ω_{14} share the same prefactor of about 10^{20} sec^{-1}, the 20% difference between ω_{13} and ω_{14} at the temperature of

this work implies that the corresponding activation energies differ by only $\frac{1}{2}\%$. The near equality of the activation energies is either a coincidence or it implies that the saddle point in $1\rightarrow3$ jumps is the same as in $1\rightarrow4$ jumps.

It is interesting to compare the rates of the three kinds of jumps with their jump lengths (see Fig. 1). The jumps of shortest distance ($1\rightarrow4$) occur most often, and the longest jumps ($1\rightarrow2$) occur least frequently. However, the intermediate jump rate (ω_{13}) is nearly equal to the fastest rate (ω_{14}), while the distance d_{13} is nearly equal to the distance d_{12} associated with the slowest rate. Thus, there is no *quantitative* relation between relative jump rates and distances.

We suppose that diffusion in benzene occurs via thermally generated vacancies, in common with other molecular solids.[25] However, the experiments performed on benzene to data offer no direct evidence of the role of vacancies. Fox and Sherwood have compared the activation energy for diffusion with the latent heat of sublimation;[5] they find a ratio $E_{act}/L_s=2.12$. This is in close agreement with the values found in the orientationally ordered molecular solids α-CO(2.13),[20] CO_2(2.17),[21] and N_2O(2.17).[26] The agreement suggests that the same mechanism is responsible for diffusion in the four materials.

CONCLUSIONS

There is now overwhelming evidence that the prefactor ω_0 describing jump diffusion in solid benzene is approximately 4×10^{20} sec^{-1}. The three NMR determinations (this work and Refs. 6 and 7) all sit within a factor of 2 of this value. The radiotracer data is four orders of magnitude higher, suggesting that pipe defects were involved. The fact that the radiotracer study found the correct activation energy implies that diffusion to the pipe defects (and not along them) was the bottleneck in the macroscopic diffusion process in that work.

The ^{13}C NMR technique used here is sensitive only to reorientations of the molecules that accompany the translational jumps. The agreement of our data with the previous proton data demonstrates that diffusion does occur by combined translational-rotational jumps, as previously proposed.[4] It has been shown here that there are three different jump rates in benzene, as allowed by the orthorhombic crystal structure. The rates of the two kinds of out-of-plane jumps (from one a-b plane to another) are nearly equal, indicating that their activation energies are within $\frac{1}{2}\%$ of each other. This seems an unusual coincidence. By comparison, the rate of in-plane jumps is substantially slower. We note that there is no simple relation between the jump rates and the lengths of the jumps; more subtle concepts are involved. It is not clear to us from the structure of benzene why the out-of-plane jumps should be the preferred path of diffusion. Nevertheless, this detailed picture of diffusion in benzene is a challenge to theories of diffusion in molecular solids.

ACKNOWLEDGMENTS

We gratefully acknowledge the support of the Jeffress Memorial Trust Fund; one of us (M.S.C) was supported in part by the Alfred P. Sloan Foundation. We appreciate several helpful conversations with Professor R. O. Simmons; Tim Williams assisted with the computer programming.

APPENDIX: LINE-SUBLATTICE ASSIGNMENT

For an arbitrary field orientation, there are four lines in the ^{13}C spectrum, one for each sublattice. The frequency of each line changes as the sample is rotated in the goniometer. The goniometer allows for rotation about a vertical axis (perpendicular to the field) as well as tilting ($\pm5°$) in the plane defined by the vertical axis and the magnetic field. By following the four resonant frequencies as the sample orientation is changed, the four lines may be assigned to the four sublattices, as described below.

The resonance frequency ω of a sublattice depends only on the orientation of the molecular normal $\hat{\mathbf{n}}$ to the field. Thus, one has for rotation about the vertical axis from Eq. (1),

$$\omega=\omega_\perp-\tfrac{1}{2}(\omega_\perp-\omega_{||})\sin^2\theta(1+\cos2\phi)\ ,$$

where θ is the angle between $\hat{\mathbf{n}}$ and the vertical, and ϕ is the azimuthal location of $\hat{\mathbf{n}}$ about the vertical. The values of $\omega_\perp$ and $\omega_{||}$ were obtained from powder spectra. The value of θ was found by orienting the sample about the vertical axis to minimize the frequency of a given line; this corresponds to $\phi=0$ because $\omega_\perp>\omega_{||}$. The ambiguity in obtaining θ from $\sin^2\theta$ (north-south hemisphere ambiguity) was resolved by tilting the sample $\pm5°$ and observing whether the frequency increased or decreased. The azimuthal location of $\hat{\mathbf{n}}$ was obtained directly from the goniometer setting corresponding to minimum frequency. It should be noted that the $\hat{\mathbf{n}}$ so determined are ambiguous with respect to inversion; this must be, given the second-rank tensor nature of chemical shifts.[17] Besides, the perpendicular to the molecular plane is also only defined to within an inversion.

The above procedure located the $\hat{\mathbf{n}}$ for each of the four lines. The angles between the $\hat{\mathbf{n}}$ were compared with those from Cox's x-ray-determined structure[1,2] and the lines assigned to sublattices, accordingly. Because of the symmetry of the crystal (*Pbca*), the sublattice assignment is *not* unique. However, given that $\omega_{12}=\omega_{34}$, $\omega_{13}=\omega_{24}$, and $\omega_{14}=\omega_{23}$ by symmetry, the assignment of the three distinct jump rates (ω_{12}, ω_{13}, and ω_{14}) from the data *is* unique.

[1]E. G. Cox, Rev. Mod. Phys. **30**, 159 (1958).
[2]E. G. Cox, D. W. J. Cruickshank, and J. A. S. Smith, Proc. R. Soc. London, Ser. A **247**, 1 (1958).
[3]R. Van Steenwinkel, Z. Naturforsch. Teil A **24**, 1526 (1969).
[4]D. E. O'Reilly and E. M. Peterson, J. Chem. Phys. **56**, 5536 (1972).
[5]R. Fox and J. N. Sherwood, Trans. Faraday Soc. **67**, 3364 (1971).

[6]F. Noack, M. Weithase, and J. von Schutz, Z. Naturforsch. Teil A **30**, 1707 (1975).
[7]M. Stohrer, F. Noack, and W. Wolfel, in *Proceedings of the XIXth Congress Ampère,* edited by H. Brunner, K. H. Hausser, and D. Schweitzer (Groupement Ampère, Geneva, 1976), p. 521.
[8]S. McGuigan, J. H. Strange, and J. M. Chezeau, Mol. Phys. **47**, 373 (1982).
[9]J. C. Brice, in *The Growth of Crystals from Liquids,* Vol. 12 of *Selected Topics in Solid State Physics,* edited by E. P. Wohlfarth (American Elsevier, New York, 1973).
[10]P. L. Kuhns and M. S. Conradi, J. Chem. Phys. **80**, 5851 (1984).
[11]P. L. Kuhns, Ph.D. thesis, College of William and Mary (1983).
[12]S. R. Hartmann and E. L. Hahn, Phys. Rev. **128**, 2042 (1962).
[13]A. Pines, M. G. Gibby, and J. S. Waugh, J. Chem. Phys. **59**, 569 (1973).
[14]G. E. Bacon, N. A. Curry, and S. A. Wilson, Proc. R. Soc. London, Ser. A **279**, 98 (1964).
[15]E. R. Andrew and R. G. Eades, Proc. R. Soc. London, Ser. A **218**, 537 (1953).
[16]C. P. Slichter, *Principles of Magnetic Resonance* (Springer, New York, 1980).
[17]M. Mehring, in *High Resolution NMR Spectroscopy in Solids,* Vol. 11 of *NMR: Basic Principles and Progress,* edited by P. Diehl, E. Fluck, and R. Kosfeld (Springer, New York, 1976).
[18]J. A. Pople, W. G. Schneider, and H. J. Bernstein, *High-Resolution Nuclear Magnetic Resonance* (McGraw-Hill, New York, 1959).
[19]E. L. Hahn, Phys. Rev. **80**, 580 (1950).
[20]S.-B. Liu and M. S. Conradi, Phys. Rev. B **30**, 24 (1984).
[21]S.-B. Liu, M. A. Doverspike, and M. S. Conradi, J. Chem. Phys. **81**, 6064 (1984).
[22]A. Abragam, *Principles of Nuclear Magnetism* (Oxford University Press, Oxford England, 1983).
[23]M. G. Gibby, A. Pines, and J. S. Waugh, Chem. Phys. Lett. **16**, 296 (1972).
[24]J. Jeener, B. H. Meier, P. Bachmann, and R. R. Ernst, J. Chem. Phys. **71**, 4546 (1979).
[25]J. N. Sherwood, in *The Plastically Crystalline State,* edited by J. N. Sherwood (Wiley, New York, 1979).
[26]K. R. Nary, P. L. Kuhns, and M. S. Conradi, Phys. Rev. B **26**, 3370 (1982).